On 2D/3D Numerical Oxidation Modeling: Calibration and Investigation of Silicon Crystal Orientation Effect on Stresses in Shallow Trench Isolations

T. Hoffmann*, K.F. Dombrowski** and V. Senez***

*IEMN-ISEN, UMR-CNRS 8520, Villeneuve d'Ascq, France, tho@isen.iemn.univ-lille1.fr
**Institute for Semiconductor Physics (IHP), Frankfurt (Oder), Germany, dombro@ihp-ffo.de
***IEMN-ISEN, UMR-CNRS 8520, Villeneuve d'Ascq, France, vsnz@isen.iemn.univ-lille1.fr

ABSTRACT

Shallow trench isolations (STI) process needs careful optimization of thermal annealings in order to minimize leakage currents which may result from excessive mechanical stresses. Due to its intrinsic three-dimensional structure, conventional 2D process simulator is no more relevant. This paper examines stress generation in STI using for the first time a 3D fully non-linear viscoelastic oxidation model implemented with the Finite Element Method.

Keywords: *isolation, viscoelasticity, raman, anisotropy.*

1. INTRODUCTION

Increased density in Si-based integrated circuits (IC) is obtained thanks to compact STI that are intrinsically three-dimensional structures. The major drawback of STI is the increase in the substrate dislocations generation due to the combined influence of mechanical stresses and high temperature processing on implantation defects [1]. Thus, eliminating these dislocations partly requires to identify and to reduce the sources of stress throughout the process. Although the measurements significantly contribute to the understanding of the stress-induced problems, they suffer from a lack of resolution (i.e., around 0.5 µm for micro-Raman profiling technique). Recently, local stress fields associated with isolation trenches have been analyzed. However, due to the extremely complex nature of the problem, the investigations were limited to two dimensions [2], or simplified three-dimensional (3D) analysis [3]. This paper examines stress generation in STI using for the first time a 3D non-linear viscoelastic oxidation model. After having demonstrated the correct prediction of the silicon dioxide shape as well as that of the stress level in the underlying substrate for different isolation structures (LOCOS and STI), the effects of oxidation on the stresses, taking into account the anisotropy of the silicon substrate, are studied revealing the value of a real 3D analysis.

2. STRESS MODELING

The initial strain condition induced by the net volume expansion of the oxidation reaction is defined by the well-known Deal and Grove law. The resulting stress profile in the entire structure is computed assuming that silicon is an elastic material while silicon dioxide (SiO_2) and nitride (Si_3N_4) are non-linear (Eyring) viscoelastic bodies. Two different methods have been developed to solve the stresses in silicon: the boundary loading (BL) and fully-integrated (FI) methods, respectively [4] (Fig. 1). The second one, more accurate, is very computationally intensive in 3D and is only used for short time oxidations. Finally, the effects of stresses on the oxidation kinetics (diffusion coefficient and reaction rate) are also included.

This oxidation model has already been implemented in our two dimensional process simulator IMPACT-4 and calibrated indirectly by reproducing accurately the shape of the most popular isolation structures [5]. In the next section, we will validate further this calibration by comparing directly the calculated and measured stresses.

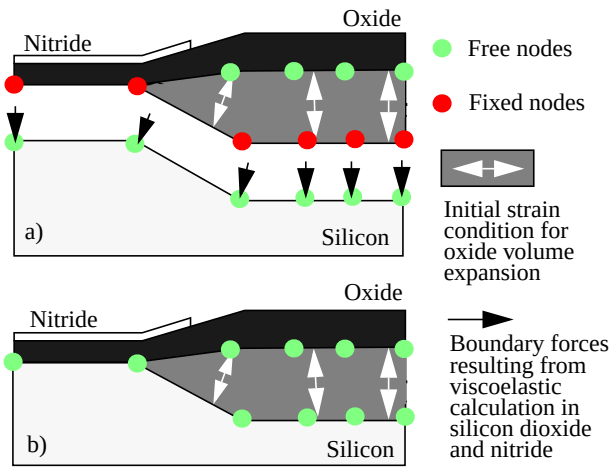

Figure 1: Schematic description of the a) boundary loaded and b) fully integrated method to calculate the stresses in silicon during an oxidation step.

The meshing task in our model can be described according to the following scheme. In an initial step, a tetrahedral mesh of the structure is generated using either MESH from ISE-AG or TETMESH from SIMULOG [6]. Then, a new SiO_2 layer of infinitesimal thickness is generated on all interfaces between oxidizable and non-oxidizable materials preventing all discontinuous or singular displacements of mesh nodes. The changes in the geometry are described by the displacement field computed during the oxidation time step. In order to keep the same mesh resolution and quality during the simulation, nodes are either introduced or deleted

from the initial mesh. If this procedure fails, a complete remeshing of the structure is performed, preceded by an improvement of the surface discretization [7].

Finally, to analyze a complete process flow, many other sources of stress need to be considered. Among them, one can simulate the *intrinsic* stress that developed during film deposition, the *thermal* stress due to thermal variation, and the *extrinsic* stress, induced by structural modifications (e.g., shrinkage during densification).

3. CALIBRATION

First of all, an accurate calibration of the model in 2D is required. Fig.2 illustrates the simulated isolation structure, together with the corresponding SEM photo.

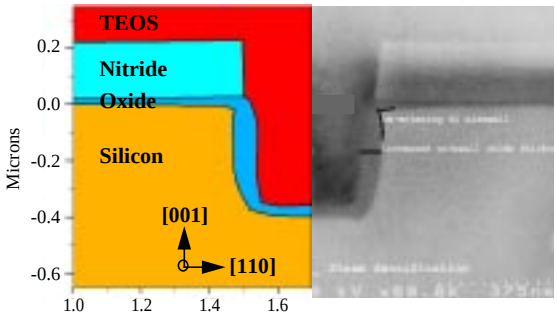

Figure 2: Simulated STI structure (left) with the corresponding SEM photo (right), after wet densification at 850°C. Silicon crystal orientations are indicated. The STI is 0.38µm deep.

The process flow is as follow: after trench etch, a 20nm sidewall oxidation is grown, followed by a 550nm LPCVD TEOS deposition and densification in wet ambient at 850˚C. We can observe from Fig.2 that the thermal oxide grown during the densification is thicker on the vertical sidewall than in the STI bottom. This is mainly due to the high oxidation rate on [110] crystallographic plane. Moreover, the simulation captures the re-entering corner effect.

Raman spectroscopy with ultraviolet excitation (UV-Raman) is used to measure the stress locally resolved [8]. Micro-Raman measurements involve focusing laser light onto a sample. Mechanical strain affects the frequencies of the Raman mode of the crystal by shifting the Raman peak. The amount and direction of the shift corresponds to the magnitude and sign of the stress (positive shift for compressive stress and negative shift for tensile stress). Fig.3 compares the measured and calculated Raman shifts after sidewall oxidation and after wet densification, for three silicon mesa widths (3µm, 2µm and 1µm). The simulation takes into account all the sources of stress (i.e., intrinsic and thermal stresses, oxidation-induced strain and TEOS densification). Due to the symmetry of the structure, only half of a pattern is simulated with appropriate boundary conditions. The high intrinsic tensile stress of the nitride film generates compression in the silicon mesa. After wet densification, the silicon consumption at the top corners induce high compressive peaks near tensile peaks coming from the nitride mask bending. The good agreement between simulation and experiment validates the model quantitatively, allowing the algorithm to be extended just as it is in 3D into DIFOX-3D.[1]

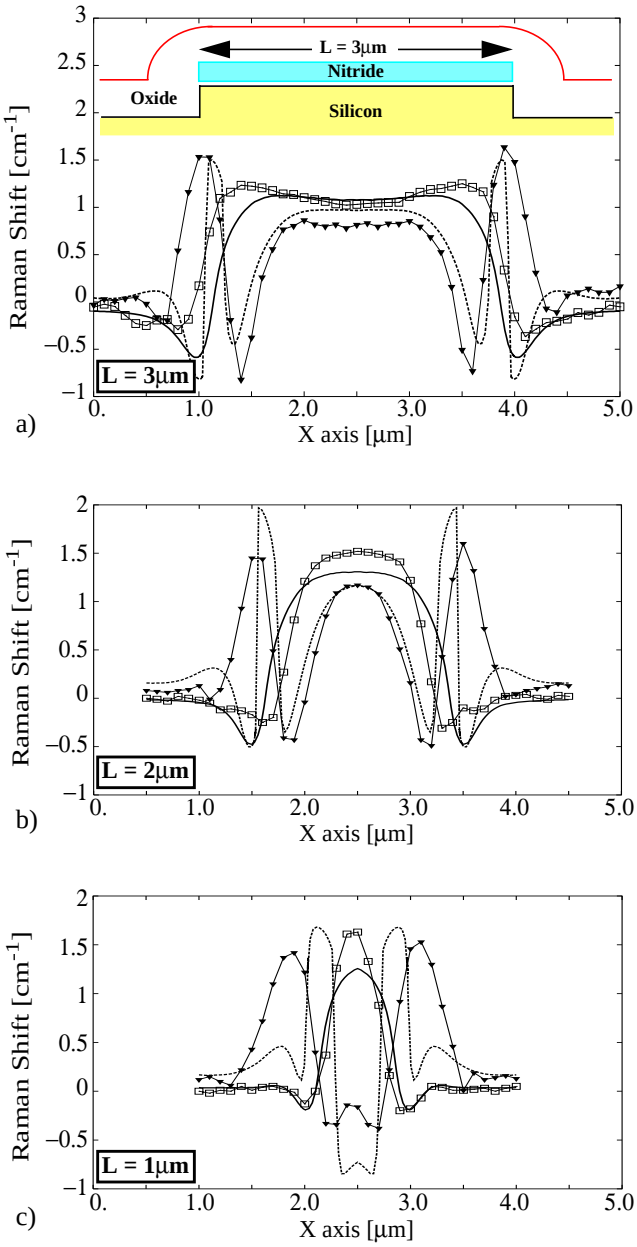

Figure 3: Comparison between simulated and measured Raman shifts, for three silicon mesa lengths: a) 3µm, b) 2µm, c) 1µm. Raman data measured at 363.7nm. After sidewall oxidation (squares: exp; full line: simulation), and after wet densification (triangles: exp; dotted line: simulation).

[1]DIFOX-3D is an home-built three-dimensional numerical code for the "hot" process steps (i.e., dopant diffusion and oxidation).

Fig.4 compares SEM measurement of a LOCOS structure with its corresponding 2D and 3D simulations, whereas Fig.5 shows the comparison between experimental and simulated Raman shifts for a slightly different LOCOS process (measurements from [9]). The results clearly indicates that the calibration is still valid in 3D, and allow us to study real 3D geometries like STI.

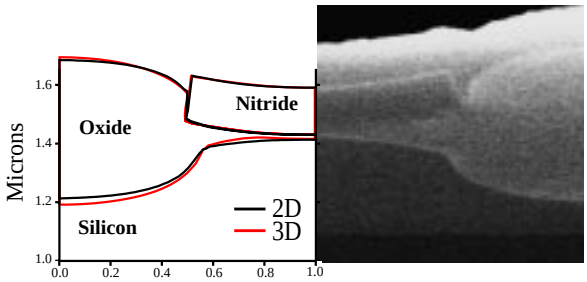

Figure 4: Comparison between SEM and simulations performed in 2D with IMPACT and in 3D with DIFOX-3D for a LOCOS structure. Nitride thickness is 160 nm, pad oxide 15 nm, oxidation performed at 920 ^{o}C during 360 minutes.

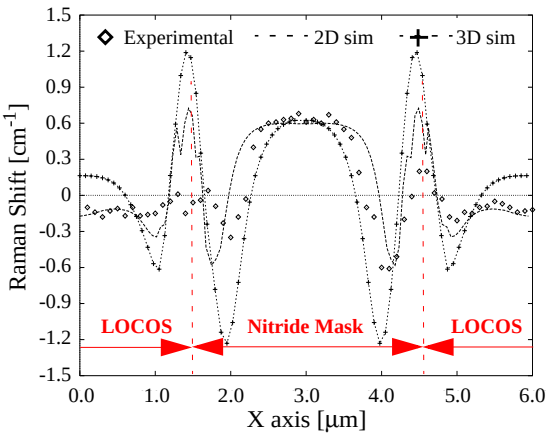

Figure 5: Comparison between simulated and measured Raman for a LOCOS structure grown at 875 ^{o}C (360 min.) with a nitride stripe of width 3.5 µm and thickness 130 nm; pad oxide of 10 nm. Raman data were measured at 457.9 nm. This result includes the intrinsic stress and the oxide growth contributions.

4. "3D" EFFECT

In this section, an application of the 3D model is presented. In order to quantify the increase of the stress in island type active areas compared to "long line" ones, different STI processes have been simulated. Fig. 6 shows the hydrostatic pressure (i.e., average of the normal stresses) distributions in two of these structures after wet densification at 850˚C. One can see that the stress is larger for square than for line and that it reaches a maximum at the edges as revealed by the 2D cross section of the line structure given in Fig. 7a. Looking at the 1D stress profiles taken at the center of the active area along the vertical direction (Fig. 7b), we notice that the stress in a square is two times larger than in a line of the same dimension. Micro-Raman measurements have confirmed this phenomenon [10]. Moreover, we observe that the compressive stress reduces once reaching the top of the active area. This phenomenon is due to the reaction to the nitride film bending. All these results demonstrate the need for a three-dimensional analysis of this isolation architecture.

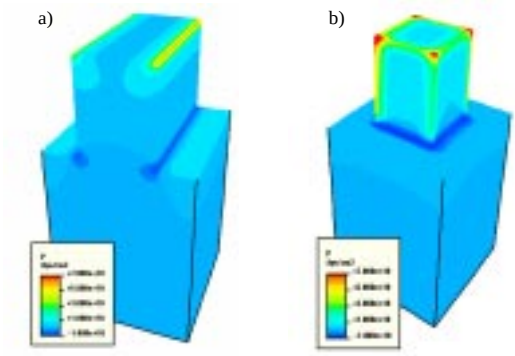

Figure 6: Comparison between a) long and b) island active areas surrounded by a shallow trench isolation. The active and isolation areas are 0.2 µm wide. The STI is 0.25 µm deep. Nitride and oxide have been removed for vizualisation.

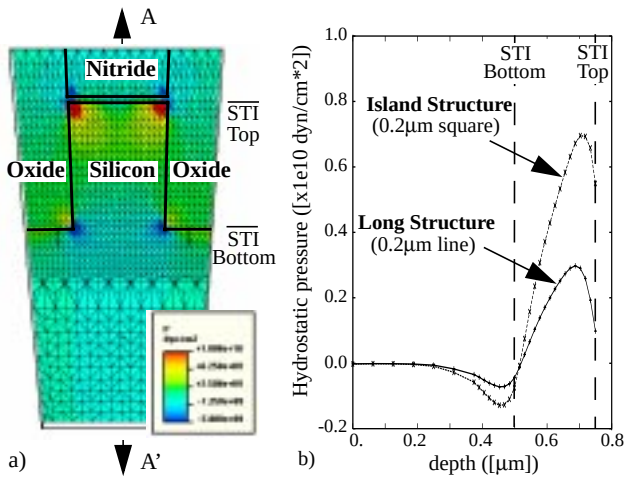

Figure 7: Comparison of the hydrostatic pressure for the 2 active areas defined in Fig. 6. a) 2D cross-section of the line structure with its pressure profile, b) 1D profiles of the pressure along the depth AA'.

5. CRYSTAL ANISOTROPY EFFECT

Finally, we investigate the effect of crystal orientations on the residual stresses for a STI structure. Indeed, Jastrzebski *et al.* [11] have demonstrated that defect generation in the vicinity of isolation structures is very sensitive to the layout orientation. Both the anisotropy of the silicon elastic tensor and the orientation-dependent oxidation rates have

been implemented. Fig.8a describes the simulated structure and Fig.8b represents the resulting hydrostatic pressure in the silicon after wet densification at 950˚C. We observe that rounding is more accentuated in the (100) plane compared to the $(01\bar{1})$ plane, due to the higher oxidation rate on (110) compared to (100) planes. However, when comparing the stresses at the Si/SiO_2 interface (Fig.9) along the directions [100], $[01\bar{1}]$ and $[11\bar{1}]$ (the diagonal), we can notice that more pronounced rounding leads to much higher compressive stresses at the top edges. Moreover, the displacement of the stress peaks from the initial edge position gives an indication of the silicon consumption at the top edges. Consequently, we can deduce from the hydrostatic pressure profiles that the silicon consumption is maximum where the nitride mask effect is the least efficient (i.e., at the "convex angle" of the nitride film along the $[11\bar{1}]$ direction).

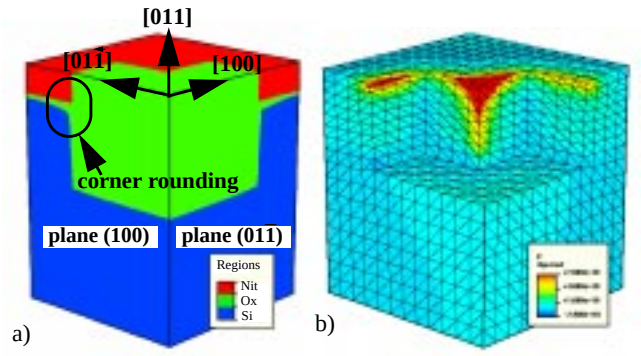

Figure 8: STI test structure (symmetrical geometry, but anisotropic crystal orientations). a) topology after $950^{o}C$ wet densification; b) Final hydrostatic pressure in the silicon.

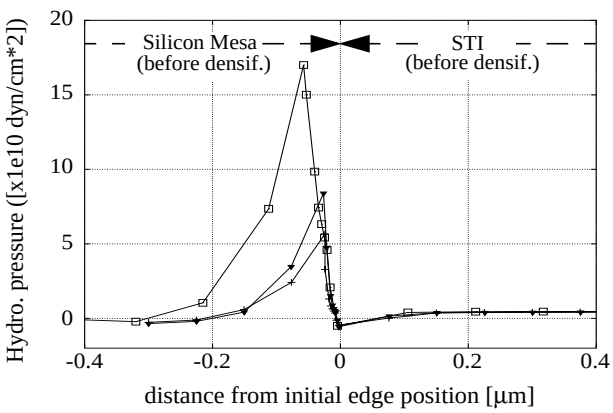

Figure 9: Silicon pressure at Si/SiO_2 interface along 3 specific directions (crosses: [100]; triangles: $[01\bar{1}]$; squares: $[11\bar{1}]$). Abscissa reference corresponds to the initial trench edge position.

6. CONCLUSION

In summary, an accurate calibration of a viscoelastic oxidation model has been obtained, by comparison with Micro-Raman and SEM structural characterization. The benefit of the extension to three dimensions, to account for effects such as those at corners in shallow trench isolation structures, has been demonstrated. Finally, by considering the anisotropy of silicon, it has been shown that the stresses can be reduced by simply changing the alignment of the pattern edges.

ACKNOWLEDGEMENTS

The authors would like to thank R. Rooyackers from IMEC (STI samples), and C. Stuer from the University of Antwerp (SEM picture). This work was part of PROMPT-II and funded as ESPRIT project 24038.

REFERENCES

[1] J. Damiano *et al.*, "*Characterization and Elimination of Trench Dislocations*", Symp. on VLSI Tech., p. 212, 1998.

[2] T. Kuroi, "*Stress Analysis of Shallow Trench Isolation for 256MDram and beyond*", IEDM Digest, p. 141, 1998.

[3] A. Poncet *et al.*, "*Simulation of Mechanical Stresses during Shallow Trench Isolation Process*", ESSDERC Proc., p. 120, 1998.

[4] H. Rueda, "*Modeling of Mechanical Stress in Silicon Isolation Technology and its Influence on Device Characteristics*", PhD dissertation, Univ. of Florida, p. 45, 1999.

[5] V. Senez *et al.*, "*Two Dimensional Simulation of Local Oxidation of Silicon: Calibrated Viscoelastic Flow Analysis*", IEEE Trans. on Electr. Devices, vol. 43-5, p. 720, 1996.

[6] TETMESH v.3.0, http://www.simulog.fr/itetmeshf.htm

[7] E. Baer *et al.*, IEEE TSM, vol. 9, no. 1, p. 67, 1996.

[8] K.F. Dombrowski *et al.*, "*Investigation of Stress in STI using UV-Raman Spectroscopy*", ESSDERC Proc., p. 196, 1999.

[9] S.K. Jones *et al.*, "*An advanced Calibration Method for Modelling Oxidation and Mechanical Stress in Sub-Micron Isolation Structures*", IEDM Digest, p. 877, 1994.

[10] I. DeWolf *et al.*, "*MicroRaman Spectroscopy Evaluation of the Local Mechanical Stress in STI CMOS Structures*", Int. Symp. for Testing & Failure Analysis (ISTFA), 1998.

[11] L. Jastrzebski *et al.*, "*Effect of Pattern Orientation on the Resistance to Process-Induced Dislocation Generation in (100) Silicon*", J. Eletrochem. Soc., vol. 134, p. 209, 1987.